



## Working Memory Classification Enhancement of EEG Activity in Dementia: A Comparative Study

Noor Kamal Al-Qazzaz\*

Sawal Hamid Bin Mohd Ali \*\*

Siti Anom Ahmad \*\*\*

\*Department of Biomedical Engineering/ Al-Khwarizmi College of Engineering/ University of Baghdad/ Baghdad / Iraq

\*\* Department of Electrical, Electronic & Systems Engineering, Faculty of Engineering & Built Environment, Universiti Kebangsaan Malaysia/ UKM Bangi/ Selangor 43600/ Malaysia  
Centre of Advanced Electronic and Communication Engineering, Department of Electrical/ Electronic and Systems Engineering/ Universiti Kebangsaan Malaysia/ Selangor 43600/ Malaysia

\*\*\*Department of Electrical and Electronic Engineering, Faculty of Engineering, Universiti Putra Malaysia, UPM Serdang/ Selangor 43400/ Malaysia  
Malaysian Research Institute on Ageing (MyAgeing™)/ Universiti Putra Malaysia/ Serdang/ Selangor 43400/ Malaysia  
Corresponding Author \*Email: [noorbme@kecbu.uobaghdad.edu.iq](mailto:noorbme@kecbu.uobaghdad.edu.iq)

\*\*Email: [sawal@ukm.edu.my](mailto:sawal@ukm.edu.my)

\*\*\*Email: [sanom@upm.edu.my](mailto:sanom@upm.edu.my)

(Received 2 January 2023; accepted 20 September 2023)

<https://doi.org/10.22153/kej.2023.09.002>

### Abstract

The purpose of the current investigation is to distinguish between working memory (*WM*) in five patients with vascular dementia (*VD*), fifteen post-stroke patients with mild cognitive impairment (*SMCI*), and fifteen healthy control individuals (*HC*) based on background electroencephalography (EEG) activity. The elimination of EEG artifacts using wavelet (WT) pre-processing denoising is demonstrated in this study. In the current study, spectral entropy (*SpecEn*), permutation entropy (*PerEn*), and approximation entropy (*ApEn*) were all explored. To improve the *WM* classification using the *k*-nearest neighbors (*kNN*) classifier scheme, a comparative study of using fuzzy neighbourhood preserving analysis with *QR*-decomposition (*FNPAQR*) as a dimensionality reduction technique and the improved binary gravitation search (*IBGSA*) optimization algorithm as a channel selection method has been conducted. The *kNN* classification accuracy was increased from 86.67% to 88.09% and 90.52% using the *FNPAQR* dimensionality reduction technique and the *IBGSA* channel selection algorithm, respectively. According to the findings, *IBGSA* reliably enhances *WM* discrimination of *HC*, *SMCI*, and *VD* participants. Therefore, WT, entropy features, *IBGSA* and *kNN* classifiers provide a valid dementia index for looking at EEG background activity in patients with *VD* and *SMCI*.

**Keywords:** Dementia, wavelet, entropy, dimensionality reduction, channels selection, features, classification.

### 1. Introduction

Stroke is broadly categorized by its type and severity and the brain region affected. Dementia can be brought on after a stroke, and its severity relies on how quickly the condition is identified and treated [1]. Following a stroke, working memory (*WM*) impairment is common. Within the

This is an open access article under the CC BY license:



first year of stroke diagnosis, vascular dementia (*VD*) may develop in 30% of stroke patients. The prevalence of *VD* doubles every 5-10 years after the age of 65 in the elderly population. Clinically speaking, mild cognitive impairment (*MCI*), in particular in attention, memory, language and orientation is a transition stage of cognitive decline [2]. At the time of diagnosis, attention, executive

functioning, and memory show the greatest impact of a stroke [3].

Patients who had suffered from cognitive impairment as a result of a stroke were the first to be introduced to the vascular cognitive impairment (VCI) spectrum, which spans the range from mild cognitive impairment (*MCI*) to advanced dementia. However, the phrase "cognitive impairment no dementia" (CIND) is used to refer to the period of time following dementia during which the brain is in danger [4]. People who have *MCI*, have a more severe decline in cognitive performance when age and education level are included, yet this decline is not as obvious in day-to-day tasks. Although some people with *MCI* will eventually develop dementia, others will remain in this *MCI* stage for a significant amount of time before progressing to dementia. Because of this, *MCI* is a disorder that can present very differently in different patients. In any case, research has been shown that patients diagnosed with *MCI* have a substantial risk of developing dementia by the third month following the onset of dementia symptoms. This risk was observed to increase significantly with time. The symptoms most commonly associated with *MCI* are those related to attention and executive function in *WM*. Daily functioning is unaffected by mild cognitive impairment. A decline in long-term memory, particularly episodic memory, is related to dementia, which is the next step following mild cognitive impairment. Mild cognitive impairment is the stage before dementia. 10% of patients will acquire post-stroke dementia (PSD) or severe dementia in the months following the commencement of an ischemic stroke (30% with recurrent ischemic stroke). This can happen as early as three months after the stroke [3].

Electroencephalography (EEG) has been extensively employed in recent years to investigate the cortical abnormalities linked to dementia and cognitive decline [5]. As a result, EEG signal analysis may reveal information on cognitive decline and dementia. Clinical EEG has a frequency range of 1 to 100 Hz and an amplitude of about 10-100 millivolts [6].

The main differences between healthy people and those with a problem with working memory (*WM*) can be summed up as follows: Dementia causes a slowing of EEG signals due to a power shift to lower frequencies and decreased cortical-subcortical communication for patients with *VD* and *SMCI*. Also, the reduction in signal complexity caused by dementia and other neurodegenerative diseases. Understanding the differences between how healthy people and people with *WM* problems show EEG signals can

help make clinical signs and better ways to diagnose neurological illnesses [5].

However, the EEG is impacted by extracranial sources known as artifacts, which can imitate the abnormal activity of the brain and hence impair the analysis. Such artifacts have been seen in EEG recordings and wrongly attributed to neurological disorders. Clinical studies involving EEG signals necessitate the creation of automatic algorithms to eliminate artifacts. Several methods have been proposed for artifact removal in the literature [7], including regression-based analysis, wavelet transform (WT), Independent Component Analysis (ICA), blind source separation (BSS), and epoch rejection. In another example of an automated hybrid artifact removal method, Al-Qazzaz et al. estimated ICs first, then used DWT to detect components as artifacts that had been marked and denoised. To produce an EEG devoid of artifacts, we correct the ICs and then reconstruct them using inv-ICA. The benefits of the proposed method were seen by the authors, who found that it improved discriminating between dementia and healthy groups [5, 8].

Numerous studies have been conducted over the past few years to examine the impact of *MCI* and AD on EEG signals and how they change over time. Using resting-state EEG recordings, Yin et al. have devised a scheme based on integrated spectral and temporal analysis for the identification of *MCI*. Stationary wavelet transform (SWT) and descriptive statistical analysis with support vector machine (SVM) classifiers were used to establish a three-dimensional discrete feature space. A machine learning-based methodology has been presented by Kashefpoor et al. to distinguish between *MCI* and normal cases utilizing basic spectral frequency band EEG data [9]. Eight EEG biomarkers, including power spectral density, skewness, kurtosis, spectral skewness, spectral kurtosis, spectral crest factor, spectral entropy, and fractal dimension, have been studied by Sharma et al. for the diagnosis of individuals with *MCI* [10]. Using the *k*-nearest neighbors (*k*NN) technique, Durongbhan et al. developed a supervised classification framework for EEG signals to distinguish between healthy controls and AD participants [11].

Previous research has largely used a 2-way classification (*AD* vs. *HC*, *SMCI* vs. *HC*) however some studies have reported using a 3-way classification. Other researchers have looked into the possibility of using power spectrum analysis for the early diagnosis of AD and *SMCI* [5]. In [12], neuro-markers based on complexity are calculated from AD patients and *HC* participants. These

complexity measures include fractal dimension and Lempel-Ziv complexity. A variety of entropies, such as spectral entropy (*SpecEn*), permutation entropy (*PerEn*), Tsallis entropy (*TsEn*), approximation entropy (*ApEn*), and sample entropy (*SampEn*), could be computed for this demand in order to examine the EEG markers that may aid in dementia early detection [13].

A three-way categorization methodology was used in one study [14]. Eyes-open, eyes-closed with a counting task, and eyes-closed conditions were used to compute spectral and complexity features from *HC*, *SMCI*, and *AD* participants, respectively. Time-frequency domain parameters (relative power band, median frequency) and entropy-based neuro-markers (spectral entropy, sample entropy, auto-mutual information) have been merged by Ruiz-Gomez et al. [15]. Eyes-open and eyes-closed EEG recordings were obtained from individuals with *AD*, *MCI*, and *HC* [16]. Classification was carried out using Linear Discriminant Analysis (LDA), Quadratic Discriminant Analysis (QDA), and Multi-layer perceptron (MLP). Toural et al. have classified patients into three groups using wavelet entropy, relative beta, and theta power [17]. In the pre-classification phase, a SVM is employed for binary assessment, and in the classification phase, a neural network is implemented for the voting mechanism. The power spectrum density of EEG sub-bands and interhemispheric coherence were determined by Oltu et al. using data from *AD*, *MCI*, and *HC*. Each EEG sub-band's variance and amplitude sum, as well as the coherence amplitude sum, are included in the feature vectors [18].

The use of EEG for the detection and classification of dementia-related brain activity patterns has shown encouraging results. In spite of this, additional study is required in two areas: dimensionality reduction and channel selection. First of all, dimensionality reduction strategies try to minimize the loss of information by simplifying the number of features or variables in EEG data. Next-generation classification algorithms can be made more manageable in terms of both complexity and computing overhead if the dimensionality of the data is reduced. The best dimensionality reduction strategies to improve EEG categorization in dementia are not yet fully understood. Despite their success elsewhere, techniques for dimensionality reduction were applied to increase the classification accuracy. There are many techniques that can be applied, including the well-known principal component analysis (PCA) technique for dimensionality reduction. The PCA approach is frequently used to

prevent redundancy in high-dimensional data [19]. Additionally, channel selection is a type of feature selection that may be applied to the removal of irrelevant or noisy channels and the selection of channels with related features [20]. The most efficient EEG channels have been determined using the sparse common spatial pattern (SCSP) algorithm, the mutual information technique [21, 22], the recursive channel elimination (RCE) approach [23], and the differential evolution – based channel selection algorithm (DEFS\_Ch) [20, 24]. Although the strategy of channel selection can offer the benefits of eliminating unimportant channels or choosing a small number of significant EEG features to enhance classification performance.

Second, channel selection includes picking the EEG channels that add the most value to the categorization process. This method can enhance classification precision, however, the best way to pick channels for EEG classification purposes in dementia is not yet certain. Channel selection can be based on a variety of parameters, including statistics, spectral analysis, and geographical patterns; nevertheless, their efficacy and robustness must be assessed in the context of dementia [25].

Most of the approaches in the literature have a complicated structure and take a long time since they do not employ a data-efficient reduction technique, which is necessary for fast and accurate analysis.

Effective dimensionality reduction approaches and optimal channel selection procedures are the last pieces of the puzzle when it comes to improving EEG classification for dementia. Closing these knowledge gaps will aid in the creation of more precise and time-saving EEG-based categorization systems for the diagnosis and monitoring of dementia. To improve EEG categorization for dementia, more study is needed to analyze and compare different ways and determine the most suitable techniques.

Based on background electroencephalography (EEG) activity, the goal of the current investigation is to differentiate between working memory (*WM*) in five patients with vascular dementia (*VD*), fifteen post-stroke patients with mild cognitive impairment (*SMCI*), and fifteen healthy control individuals (*HC*). In the current study, as spectral entropy (*SpecEn*), permutation entropy (*PerEn*) and approximation entropy (*ApEn*), were the features that were selected to investigate the *WM* and classify their tasks using the k-nearest neighbours (*kNN*) classifier scheme. Therefore, a comparative study of using the fuzzy neighborhood

preserving analysis with  $QR$ -decomposition ( $FNPAQR$ ) as a dimensionality reduction technique and the improved binary gravitation search ( $IBGSA$ ) optimization algorithm as a channel selection method has been conducted. The  $FNPAQR$  was used in this investigation as a dimensionality reduction method to maximize the distance between the centers of various classes while minimizing the distance between samples that belong to the same class [26, 27]. Additionally, the most efficient channels that increase classification accuracy have been found using the  $IBGSA$  algorithm [25]. Additionally, the suitability of  $SpecEn$ ,  $ApEn$ , and  $PerEn$  characteristics for the early identification of  $VD$  was examined.  $kNN$  classifier has also been used to identify patients with post-stroke  $WM$  dysfunction.

## 2. Materials and Methods

To improve the  $WM$  classification of dementia patients, the EEG signals would undergo various signal processing phases, as shown in Figure 1. The participants in this EEG study participated in a session of an auditory  $WM$  task. The non-stationary EEG signals were initially processed using a wavelet (WT) denoising approach during the preprocessing step. After that, we look into and extract the meaningful features, such as non-linear  $SpecEn$ ,  $ApEn$ , and  $PerEn$  entropy features, and conduct a comparison of the dimensionality reduction techniques fuzzy neighborhood preserving analysis with  $QR$ -decomposition ( $FNPAQR$ ) and the improved binary gravitation search ( $IBGSA$ ) optimization algorithm for channel selection. Finally, the performance of the classifiers utilized is evaluated, showing that dementia classification techniques can be used to categorize patients' mental disability after stroke.

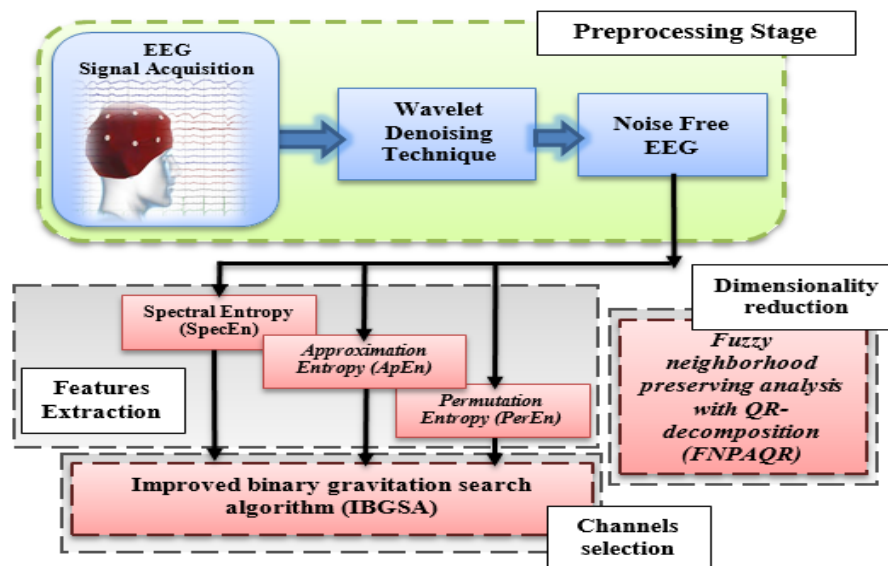


Fig. 1. The block diagram of the proposed study.

### 2.1 Participants

In the current investigation, 35 patients' EEG datasets were examined. The sample was recruited from the stroke unit and neurology clinic at the Pusat Perubatan Universiti Kebangsaan Malaysia (PPUKM). 15  $HC$  participants (7 male and 8 female, age  $60.06 \pm 5.21$ ), 15  $SMCI$  patients (5 male and 10 female, age  $60.26 \pm 7.77$ ), and 5  $VD$  patients (3 male and 2 female, age  $64.6 \pm 4.8$ ) had their EEG data reviewed. The cognitive evaluations that were administered to the three groups were the mini-mental state examination

(MMSE) [7] and the Montreal cognitive assessment (MoCA) [8].  $HC$  participants' MMSE and MoCA scores were ( $29.6 \pm 0.73, 29.06 \pm 0.88$ ), but  $SMCI$  patients' MMSE and MoCA scores were ( $20.2 \pm 5.63$  and  $16.13 \pm 5.97$ ), respectively. Lastly, the MMSE and MoCA scores for the  $VD$  patients were ( $14.8 \pm 1.92$  and  $14.8 \pm 1.92$ ) respectively. The experimental methods utilized throughout the research were approved by PPUKM's Human Ethics Committee, and the patients' voluntary and informed consent was secured by acquiring signed consent forms. All patients were diagnosed using computed

tomography/magnetic resonance imaging (CT/MRI) scans, patient medical histories, and clinical and laboratory tests.

## 2.2 EEG recording

NicoletOne (V32) was utilized in order to collect the 19 EEG channel datasets. Using a single ground electrode and two reference electrodes with 19 channels starting from left, right to the center, these are: Fp2, F8, T4, T6, O2, Fp1, F7, T3, T5, O1, F4, C4, P3, F3, C3, P3, Fz, Cz and Pz.

A referential montage was created, and the channels were constructed according to the 10-20 international framework. The Nicolet EEG system was sampled at 256 Hz, and the electrode-skin impedance was tested to ensure that it did not exceed 10 kilo ohms. This corresponded to a sensitivity of 100 v/cm, whereas the low cut-off frequency and high cut-off frequency were, respectively, 0.5 Hz and 70 Hz. The EEG was recorded for 60 seconds, with a 0.5-second fixation cue preceding the start of the recording period. The patients were then asked to commit five words to memory for 10 seconds as part of a simple auditory WM test involving working memory. Following this, EEG recordings were made as each subject attempted to recall the phrase. After the 60-second interval elapsed, the researcher instructed the participants of the sample group to open their eyes and to recall in turn each of the words they had memorized [3].

## 2.3 Preprocessing Stage

In this investigation, WT denoising was utilized to eliminate EEG artifacts. Since the sampling frequency was 256 Hz [28], the symlets mother WT of order 9 'sym9' and 5 decomposition levels were utilized to decompose the acquired EEG information.

As in Equation 1, the discrete values of  $a$  and  $b$  can process the DWT. It can be constructed as a set of decomposition functions of the correlation between the signal  $f(t)$  and the shifting and dilating of the mother wavelet function  $\psi(t)$ . In Equation 2, location parameter  $b$  shifts MWT and the frequency scaling parameter  $a$  dilates or contracts it [29, 30]:

$$\begin{aligned} DWT_{m,n}(f) &= a_0^{-m/2} \int f(t) \psi(a_0^{-m}t - nb_0) dt \\ a_0 \text{ and } b_0 \text{ values are set to 2 and 1, respectively.} \end{aligned}$$

$$\begin{aligned} \psi_{a,b}(t) &= \frac{1}{\sqrt{a}} \psi\left(\frac{t-b}{a}\right), a \in \mathbb{R}^+, b \in \mathbb{R} \end{aligned} \quad \dots (2)$$

## 2.4 Features Extraction Stage

Each EEG dataset had 19 channels with a duration of 60 seconds, so 15360 samples were utilized for this study. Entropies have been utilized to identify anomalies in dementia patients' EEGs. The EEGs of dementia patients have been separated from those of age-matched healthy people using *SpecEn* [31-33].

After normalizing the power spectral density (*PSD*) to a scale from 0 to 1 to obtain normalized PSD ( $PSD_n$ ), which has the value 1 for  $\sum PSD_n(f) = 1$ , the *SpecEn* is computed as in Equation 3 [31].

$$\begin{aligned} SpecEn &= \frac{-1}{\log(N)} \sum_{f=0.1Hz}^{64Hz} PSD_n(f) \log[PSD_n(f)] \end{aligned} \quad \dots (3)$$

Utilizing the algorithm described in [34], *ApEn* is calculated as in Equation 4 [35].

$$ApEn(m, r, N) = \phi^m(r) - \phi^{m+1}(r) \quad \dots (4)$$

where,  $\phi^m$  is the natural logarithm for  $m$  contiguous observation within tolerance width  $r$  and  $N$  is the number of points of the EEG time series. For the sake of our analysis, *ApEn* is calculated with a tolerance of  $r = 0.2 \times SD$  and a run length of  $m = 2$  epochs, where  $SD$  is the standard deviation.

In the case of *PerEn*, this sort of entropy is widely employed in the context of artefacts and noise, and one of its distinguishing properties [36] is its computational speed.

In terms of *PerEn*'s applications, non-stationary and non-linear signals are frequently employed [37]. *PerEn* has been utilized by researchers to assess the complexity of EEG signals in Alzheimer's disease (AD) patients [38]. The *PerEn* can also be used to detect aberrant electrical activity in the brain, which cannot be demonstrated by traditional EEG signal detection methods [39].

When all motifs have equal probability, the largest value of *PerEn* is obtained, which has a value of  $\ln d!$ , where  $d = 3, l = 1$ . In contrast, if there is only one  $p(\pi_k)$  different from zero, which illustrates a completely regular signal, the smallest value of *PerEn* is obtained as much as 0 [36, 40, 41]. For 60 seconds,  $N = 15360$  samples, 6 windows of 10 second length (2560 samples)

were extracted from the original EEG time series for each of 19 channels.

In order to estimate the *PerEn*, assume the time series of  $y = \{y_1, y_2, \dots, y_N\}$  of length  $N$ , at each time  $t$  of  $y$  a vector including the  $d^{th}$  subsequence value constructed as:  $Y_t^{d,l} = \{y_t, y_{t+1}, \dots, y_{t+(d-2)l}, y_{t+(d-1)l}\}$  for  $t = 1, 2, \dots, N - (d-1)l$ , where  $d$  is the embedded dimension, determines how much information is contained in each vector and  $l$  is the time delay. To calculate the *PerEn*, the  $d$  of  $y_i$  are associated with numbers from 1 to  $d$  and arranged in increasing order as  $\{y_{t+(j_1-1)l}, y_{t+(j_2-1)l}, \dots, y_{t+(j_{d-1}-1)l}, y_{t+(j_d-1)l}\}$  for different samples, there will be  $d!$  potential ordinal patterns,  $\pi$ , which are named “motifs” [38]. For each  $\pi_t$ ,  $p(\pi_t)$  demonstrate the relative frequency as follows:

$$p(\pi_i^{d,l}) = \frac{\#\{t|t \leq N-d, \text{type}(Y_t^{d,l}) = \pi_i^{d,l}\}}{N-d+1} \quad \dots(5)$$

Where  $\#\{ \}$  denotes the cardinality of the set (the number of elements). The *PerEn* is computed as follows:

$$H(y, d, l) = - \sum_{\pi_k=1}^{\pi_k=d!} p(\pi_k) \ln p(\pi_k) \quad \dots(6)$$

When all motifs have equal probability, the largest value of *PerEn* is obtained, which has a value of  $\ln d!$ , where  $d = 3, l = 1$ . In contrast, if there is only one  $p(\pi_k)$  different from zero, which illustrates a completely regular signal, the smallest value of *PerEn* is obtained as much as 0 [36, 40, 41]. For 60 seconds,  $N = 15360$  samples, 6 windows of 10 second length (2560 samples) were extracted from the original EEG time series for each 19 channels.

## 2.5 Statistical analysis

The denoised 19 channels from the EEG dataset of 15 *HC*, 15 *SMCI*, and 5 *VD* patients were preliminary divided into 5 recording regions that correspond to the scalp area of the cerebral cortex. The frontal includes seven channels: Fp1, Fp2, F3, F4, F7, F8 and Fz, temporal includes four channels: T3, T4, T5 and T6, parietal includes three channels: P3, P4 and Pz), occipital includes two channels: O1 and O2), and central includes three channels: C3, C4 and Cz). The Kolmogorov–Smirnov test determined normality, while Levene's test confirmed homoscedasticity. Thus, SPSS 22 used two analysis of variance (ANOVA) sections on *SpecEn*, *ApEn*, and *PerEn* characteristics. Each segment had two independent variables (IVs): the subject groups (*HC* subjects, *SMCI*, and *VD* patients) and the five scalp regions (frontal,

temporal, parietal, occipital, and central). One of the former attributes was the dependent variable (DV). All statistical tests were significant at  $P < 0.05$ .

## 2.6 Dimensionality reduction using FNPAQR

In order to maximize the distance between the centers of various classes while minimizing the distance between samples that belong to the same class, this study also used the fuzzy neighborhood preserving analysis with QR-decomposition (*FNPAQR*) dimensionality reduction technique [26] of Khushaba et al [20]. *FNPAQR* maintains the contribution of samples to various classes in this way [26]. For the first time, our study used *FNPAQR* to distinguish between *HC* and demented participants during *WM* tasks.

The matrix ( $G_{FNPAQR}$ ) was built from the training set to project the input feature vector using *FNPAQR*. To reduce dimensionality, the projection matrix was multiplied by the training and testing sets. *FNPAQR* projected training data input feature vector. Projecting the feature vector's testing set requires merely multiplying it by the projection matrix from the training data. Figure 2 shows how the *FNPAQR* feature projection calculates the within-class scatter matrix ( $S_W$ ) and between-class scatter matrix ( $S_B$ ). calculates the within-class scatter matrix ( $S_W$ ) and between-class scatter matrix ( $S_B$ ).

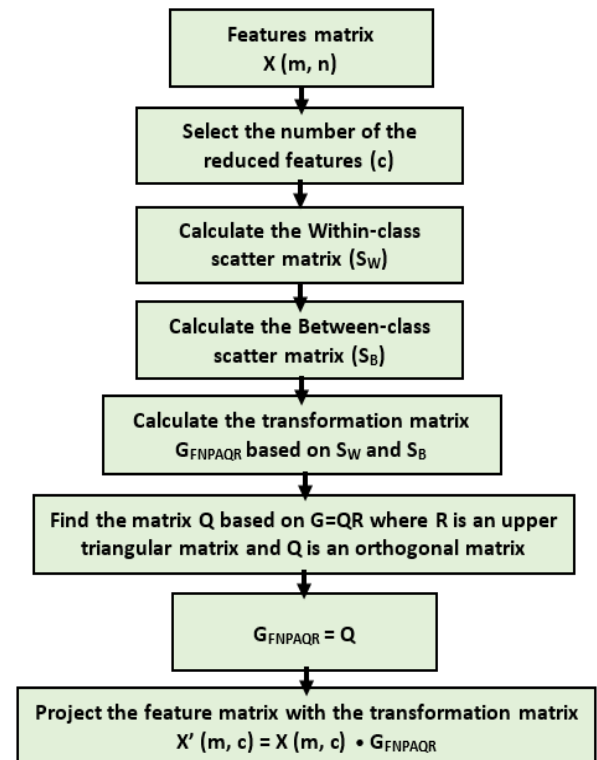


**Fig. 2. The steps of Dimensionality reduction using FNPAQR**

In a comparative study, the *FNPAQR* dimensionality reduction approach and *k* NN classifier were used to identify *VD*, *SMCI*, and *HC* subjects [5].

## 2.7 Channel Selection using IBGSA

The most effective channels have been found, and the amount of information has been decreased, using the improved binary gravitation search algorithm (*IBGSA*) optimization algorithm [25, 42]. *GSA* is a powerful optimization technique that was first proposed in [43]. for use in addressing binary-valued problems. It was created based on the Newtonian laws of gravity and motion. *N* objects (agents) are defined for the *IBGSA* algorithm to determine the best EEG channels. The population starts out with this collection of things. Each object in this study is regarded as a binary vector with a dimension of 19. The number of EEG channels is the same as the dimension that was given. The following vector can be regarded as the  $i^{th}$  object. Finding the item that gives the best fitness value is the main objective. Equation 7 [44] can be used to calculate the classification accuracies for each set of EEG channels, which are used in this work to determine the *fitness* values for the objects:

$$fit_i = \omega_1 \times accu_i + \omega_2 \times \left[ 1 - \frac{\sum_{j=1}^p f_j}{p} \right]$$

where  $\omega_1, \omega_2$  are predefined weight factors,  $\omega_1$  is the weight factor for the classification accuracy of the *k* NN classifiers respectively determined by the 10-fold cross-validation (*CV*) method;  $accu_i$  is the 1-NN classification accuracy;  $\omega_2$  is the weight factor for the number of selected features and  $f_j$  is the value of the feature mask. If precision is the most crucial factor, the *weight* factor might be increased to a high amount (such as 100%). The position of the object with a high fitness value should be set suitably since it has a high likelihood of influencing the positions of the other objects in the following iteration [14,15]. Equation 8 yields the  $accu_i$ , where *corr* is the number of cases that were properly classified and *incorr* is the number of examples that were classified wrongly [44]:

$$accu_i = \frac{corr}{corr+incorr} \times 100\% \quad \dots(8)$$

The *IBGSA* algorithm selects the most informative EEG channels for classification. The method selects the optimal EEG channel subset for classification. The technique optimizes channel selection to increase EEG-based classification accuracy and efficiency [43].

## 2.8 Dementia Classification Techniques

The EEG signals were divided into (*HC*, *SMCI*, and *VD*) using a *k*NN classifier. The patients with *VD* made up a statistically significant minority in this analysis. To address the discrepancy, the researchers used a synthetic oversampling technique (*SMOTE*) [45]. To prevent overfitting and bias in the classification analysis, the classifier parameters and the percentage of oversampling were evaluated by 10-fold cross-validation with a grid search approach [46]. The provided data set was partitioned into ten independent samples of similar size. Only one of these groups was utilized to train the classifier, while the other nine were used as the test set. Ten iterations of this process yielded ten reliable results. The 10-fold *CV* accuracy of this dataset was calculated as the mean of these accuracies [47].

Since *SMOTE* modifies the dataset, the oversampling was incorporated into the settings. Because of this, it is possible that the parameters discovered with varying amounts of *SMOTE* are not equivalent. When using the *SMOTE* to normalize the class frequencies, we solely considered the training set [48, 49].

The classifier in this study was trained to find the best value of *k*, which was discovered to be *k* = 5, and to increase classification accuracy. Each trial has been classified by *k*NN using the Euclidean distance as a similarity metric.

After selecting the optimal EEG channels, the *k*NN algorithm classifies background signals from symptomatic and asymptomatic instances using entropy. *k*NN uses labeled training samples to classify data points. EEG signal entropy measures randomness or chaos. The *k*NN method classifies symptomatic and asymptomatic cases based on their resemblance to training samples by computing the entropy of chosen EEG channels [50].

## 3. Results and Discussion

### 3.1 Results of Preprocessing Stage

Figure 3 depicts the denoised EEG signals produced by the *WT* method. Due to the heterogeneity of EEG artifacts, *WT* has been

evaluated on every channel of the available EEG datasets. When comparing the original recorded EEG (red) with the suppressed version (blue), it is

clear that the artifactual components were effectively eliminate

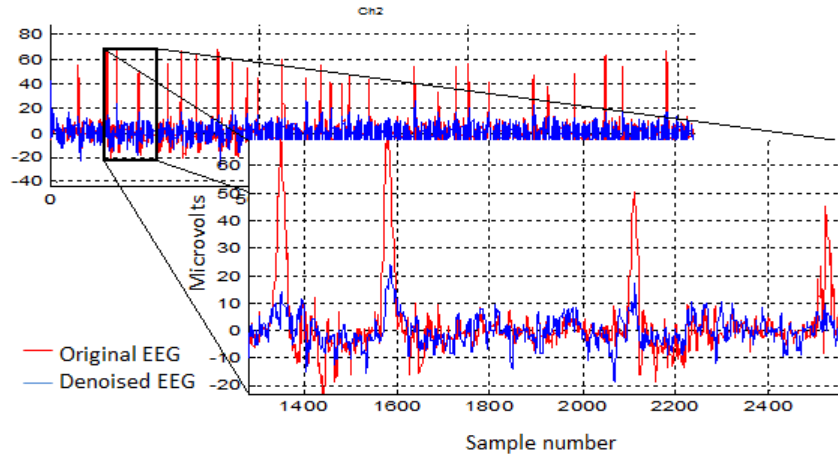


Fig. 3. The denoising resulting from the application of the WT technique to EEG Ch2 which represents F8.

### 3.2 Results of Statistical analysis

Patients with *VD* showed less complexity than those with *SMCI* and *HC* using *SpecEn*, *ApEn* and *PerEn* as shown in Figures 4, 5 and 6. For all patients, but especially for those with *HC* and *VD*, the complexity of the EEG signals reduces as the condition worsens.

Figure 4 shows that the *SpecEn* values of the *VD* patients were lower than those of the *SMCI* patients and that the *HC* patients' values were the greatest.

Moreover, the *VD* patients had lower *ApEn* values than the *SMCI* patients, and the *HC* subjects had the highest *ApEn* values (Figure 5). Finally, the patients with *VD* had lower *PerEn* values than those with *SMCI*, and the participants with *HC* had the greatest value (Figure 6).

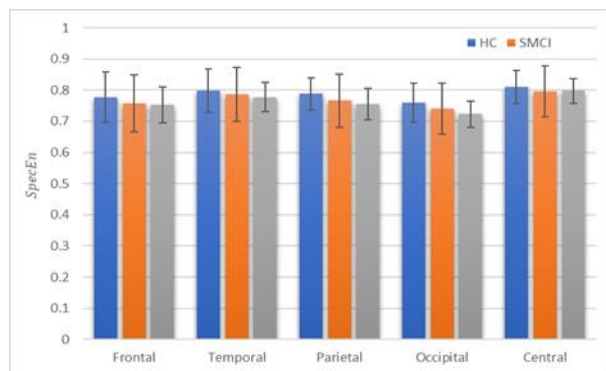


Fig. 4. Comparative plot of the *SpecEn* for the five scalp regions of the brain for *VD*, *SMCI* patients and *HC* subjects.

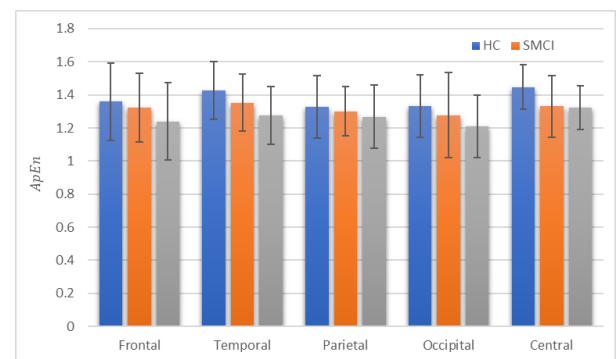


Fig. 5. Comparative plot of the *ApEn* for the five scalp regions of the brain for *VD*, *SMCI* patients and *HC* subjects.

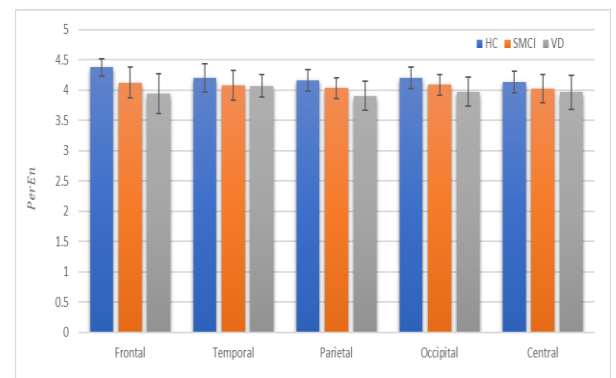


Fig. 6. Comparative plot of the *PerEn* for the five scalp regions of the brain for *VD*, *SMCI* patients and *HC* subjects.

### 3.3 Results of Dementia Classification Techniques

The classification confusion matrix for all three schemes proposed is shown in Tables I, II and III. Table I illustrates the confusion matrix for the  $k$ NN Classifier without using the *FNPAQR* and *IBGSA*. Table II shows the confusion matrix for the  $k$  NN Classifier with the *FNPAQR* dimensionality reduction technique. The number of selected features by the *FNPAQR* dimensionality reduction technique was set to 40 characteristics, which are the most essential features in terms of differentiating between patients suffering from *VD* and stroke-related *SMCI* and healthy control participants. Table III shows the confusion matrix for the  $k$ NN Classifier with the *IBGSA* channels selection algorithm. The  $k$  NN classification accuracy was improved from 86.67% to 88.09 using *FNPAQR* dimensionality reduction technique and 90.52 by *IBGSA* channel selection algorithm. The results suggested that *IBGSA* consistently improves *WM* discrimination of *VD*, *SMCI* patients and *HC* subjects. Therefore, *IBGSA* improves the classification over all accuracy for all three groups as in the  $k$  NN classification over the *FNPAQR* accuracy.

**Table 1,**  
Calculation of the confusion matrix for multi-class classification using the  $k$ NN Classifier.

confusion matrix	VD	SMCI	HC
<i>VD</i>	93.33%	6.67%	0.00%
<i>SMCI</i>	5.56%	93.33%	1.11%
<i>HC</i>	16.67%	10%	73.33%

**Table 2,**  
Calculation of the confusion matrix for multi-class classification using  $k$ NN and the *FNPAQR* technique.

confusion matrix	VD	SMCI	HC
<i>VD</i>	87.78%	11.11%	1.11%
<i>SMCI</i>	7.78%	92.22%	0.00%
<i>HC</i>	6.67%	16.67%	76.67%

**Table 3,**  
Calculation of the confusion matrix for multi-class classification using  $k$ NN and the *IBGSA* technique.

confusion matrix	VD	SMCI	HC
<i>VD</i>	67.78%	31.11%	1.11%
<i>SMCI</i>	7.78%	88.89%	3.33%
<i>HC</i>	3.33%	6.67%	90%

As a result,  $k$ NN was used in the study to support multi-class classification and to distinguish *VD*, *SMCI* patients, and *HC* subjects. This study had several limitations, including a small sample size, and an additional analysis with a large database should be performed in the future.

Finally, we compared the proposed approach to other cutting-edge methods in the literature that employed the different dementia datasets as we did in our work. The results show that our model outperforms other existing methods in the literature, with the highest classification accuracy of 90.52% compared to Kashefpoor et al. [9] proposed a methodology that obtained an accuracy of around 88%, Sharma et al. [10] investigated different features for control vs. *MCI* signal classification and obtained accuracy ranges between 73.2% and 89.8%.

## 4. Conclusion

The electroencephalogram (EEG) is a vital tool for studying mental processes. Here, we analyze and filter EEG signals to identify promising channels and useful markers for an earlier, more accurate diagnosis of dementia. The WT method has been implemented as a denoising method. Patients with *VD* and *SMCI* have had their irregularities assessed with *SpecEn*, *ApEn*, and *PerEn* as characteristics. To improve *WM* categorization, we applied the *FNPAQR* dimensionality reduction technique in conjunction with the *IBGSA* channel selection algorithm. *FNPAQR* dimensionality reduction technique increased  $k$  NN classification accuracy from 86.67% to 88.09%, while the *IBGSA* channel selection algorithm increased it to 90.52%. Findings revealed that *IBGSA* reliably enhances *WM* discrimination in *VD*, *SMCI* patients, and *HC* controls. Because of these findings, it is clear that minimizing the number of channels used in the *IBGSA* selection process has a substantial impact on improving classification accuracy.

Working memory stores and manipulates information for ongoing tasks. Dementia causes cognitive deterioration, including working memory loss. Therefore, working memory enhancement may slow dementia-related cognitive deterioration. Working memory training may increase brain activity in working memory-related areas, however, healthy volunteers trained working memory using an adaptive N-back task. The training did not directly cause changes in brain activation in several important locations. In spite of that, studies have

implied that working memory training may have benefits, but more study is needed to determine the long-term consequences. Working memory training alone may not diminish dementia-related brain activity since dementia is complicated. Working memory training may also be affected by dementia stage, type, and training procedure. In general, improving working memory in people who have dementia continues to be our focus of research. Future studies may provide additional insights into effective interventions and techniques to improve cognitive function and quality of life.

## References

- [1] B. C. Campbell, D. A. De Silva, M. R. Macleod, S. B. Coutts, L. H. Schwamm, S. M. Davis, *et al.*, "Ischaemic stroke," *Nature Reviews Disease Primers*, vol. 5, p. 70, 2019.
- [2] N. K. Al-Qazzaz, S. H. Ali, S. A. Ahmad, and S. Islam, "Cognitive assessments for the early diagnosis of dementia after stroke," *Neuropsychiatric disease and treatment*, vol. 10, p. 1743, 2014.
- [3] N. K. Al-Qazzaz, S. H. Ali, S. A. Ahmad, S. Islam, and K. Mohamad, "Cognitive impairment and memory dysfunction after a stroke diagnosis: a post-stroke memory assessment," *Neuropsychiatric disease and treatment*, vol. 10, p. 1677, 2014.
- [4] C. N. Kan, J. Cano, X. Zhao, Z. Ismail, C. L.-H. Chen, and X. Xu, "Prevalence, clinical correlates, cognitive trajectories, and dementia risk associated with mild behavioral impairment in Asians," *The Journal of Clinical Psychiatry*, vol. 83, p. 40123, 2022.
- [5] N. K. Al-Qazzaz, S. H. B. M. Ali, S. A. Ahmad, M. S. Islam, and J. Escudero, "Discrimination of stroke-related mild cognitive impairment and vascular dementia using EEG signal analysis," *Medical & biological engineering & computing*, vol. 56, pp. 137-157, 2018.
- [6] N. K. Al-Qazzaz, S. H. B. Ali, S. A. Ahmad, K. Chellappan, M. S. Islam, and J. Escudero, "Role of EEG as Biomarker in the Early Detection and Classification of Dementia," *The Scientific World Journal*, vol. 2014, 2014.
- [7] E. H. Houssein, A. Hammad, and A. A. Ali, "Human emotion recognition from EEG-based brain-computer interface using machine learning: a comprehensive review," *Neural Computing and Applications*, vol. 34, pp. 12527-12557, 2022.
- [8] N. K. Al-Qazzaz, S. Hamid Bin Mohd Ali, S. A. Ahmad, M. S. Islam, and J. Escudero, "Automatic artifact removal in EEG of normal and demented individuals using ICA-WT during working memory tasks," *Sensors*, vol. 17, p. 1326, 2017.
- [9] M. Kashefpoor, H. Rabbani, and M. Barekatin, "Automatic diagnosis of mild cognitive impairment using electroencephalogram spectral features," *Journal of medical signals and sensors*, vol. 6, p. 25, 2016.
- [10] N. Sharma, M. Kolekar, K. Jha, and Y. Kumar, "EEG and cognitive biomarkers based mild cognitive impairment diagnosis," *Irbm*, vol. 40, pp. 113-121, 2019.
- [11] P. Durongbhan, Y. Zhao, L. Chen, P. Zis, M. De Marco, Z. C. Unwin, *et al.*, "A dementia classification framework using frequency and time-frequency features based on EEG signals," *IEEE Transactions on Neural Systems and Rehabilitation Engineering*, vol. 27, pp. 826-835, 2019.
- [12] A. H. H. Al-Nuaimi, E. Jammeh, L. Sun, and E. Ifeachor, "Complexity measures for quantifying changes in electroencephalogram in Alzheimer's disease," *Complexity*, vol. 2018, 2018.
- [13] N. K. Al-Qazzaz, M. K. Sabir, A. H. Al-Timemy, and K. Grammer, "An integrated entropy-spatial framework for automatic gender recognition enhancement of emotion-based EEGs," *Medical & Biological Engineering & Computing*, pp. 1-20, 2022.
- [14] M. Şeker, Y. Özbek, G. Yener, and M. S. Özerdem, "Complexity of EEG dynamics for early diagnosis of Alzheimer's disease using permutation entropy neuromarker," *Computer Methods and Programs in Biomedicine*, vol. 206, p. 106116, 2021.
- [15] S. J. Ruiz-Gómez, C. Gómez, J. Poza, G. C. Gutiérrez-Tobal, M. A. Tola-Arribas, M. Cano, *et al.*, "Automated multiclass classification of spontaneous EEG activity in Alzheimer's disease and mild cognitive impairment," *Entropy*, vol. 20, p. 35, 2018.
- [16] C. S. Musaeus, K. Engedal, P. Høgh, V. Jelic, M. Mørup, M. Naik, *et al.*, "EEG theta power is an early marker of cognitive decline in dementia due to Alzheimer's disease," *Journal of Alzheimer's Disease*, vol. 64, pp. 1359-1371, 2018.
- [17] J. E. Santos Toural, A. Montoya Pedrón, and E. J. Marañón Reyes, "Classification among healthy, mild cognitive impairment and Alzheimer's disease subjects based on wavelet entropy and relative beta and theta power," *Pattern Analysis and Applications*, vol. 24, pp. 413-422, 2021.

- [18] B. Oltu, M. F. Akşahin, and S. Kibaroglu, "A novel electroencephalography based approach for Alzheimer's disease and mild cognitive impairment detection," *Biomedical Signal Processing and Control*, vol. 63, p. 102223, 2021.
- [19] M. KavitaMahajan and M. S. M. Rajput, "A Comparative study of ANN and SVM for EEG Classification," *International Journal of Engineering*, vol. 1, 2012.
- [20] N. K. Al-Qazzaz, S. H. M. Ali, and S. A. Ahmad, "Differential Evolution Based Channel Selection Algorithm on EEG Signal for Early Detection of Vascular Dementia among Stroke Survivors," in *2018 IEEE-EMBS Conference on Biomedical Engineering and Sciences (IECBES)*, 2018, pp. 239-244.
- [21] T. Lan, D. Erdogmus, A. Adami, S. Mathan, and M. Pavel, "Channel selection and feature projection for cognitive load estimation using ambulatory EEG," *Computational intelligence and neuroscience*, vol. 2007, pp. 8-8, 2007.
- [22] M. Arvaneh, C. Guan, K. K. Ang, and C. Quek, "Optimizing the channel selection and classification accuracy in EEG-based BCI," *IEEE Transactions on Biomedical Engineering*, vol. 58, pp. 1865-1873, 2011.
- [23] M. Schröder, T. N. Lal, T. Hinterberger, M. Bogdan, N. J. Hill, N. Birbaumer, *et al.*, "Robust EEG channel selection across subjects for brain-computer interfaces," *EURASIP Journal on Applied Signal Processing*, vol. 2005, pp. 3103-3112, 2005.
- [24] N. K. Al-Qazzaz, M. K. Sabir, S. Ali, S. A. Ahmad, and K. Grammer, "Effective EEG Channels for Emotion Identification over the Brain Regions using Differential Evolution Algorithm," in *2019 41th Annual International Conference of the IEEE Engineering in Medicine and Biology Society (EMBC)*, 2019.
- [25] N. K. Al-Qazzaz, S. H. B. M. Ali, S. A. Ahmad, and J. Escudero, "Optimal EEG Channel Selection for Vascular Dementia Identification Using Improved Binary Gravitation Search Algorithm," in *International Conference for Innovation in Biomedical Engineering and Life Sciences*, 2017, pp. 125-130.
- [26] R. N. Khushaba, S. Kodagoda, D. Liu, and G. Dissanayake, "Electromyogram (EMG) based fingers movement recognition using neighborhood preserving analysis with QR-decomposition," in *Intelligent Sensors, Sensor Networks and Information Processing (ISSNIP), 2011 Seventh International Conference on*, 2011, pp. 1-105.
- [27] N. K. Al-Qazzaz, S. Ali, S. A. Ahmad, and J. Escudero, "Classification enhancement for post-stroke dementia using fuzzy neighborhood preserving analysis with QR-decomposition," in *2017 39th Annual International Conference of the IEEE Engineering in Medicine and Biology Society (EMBC)*, 2017, pp. 3174-3177.
- [28] N. K. Al-Qazzaz, S. Ali, S. Islam, S. Ahmad, and J. Escudero, "EEG Wavelet Spectral Analysis During a Working Memory Tasks in Stroke-Related Mild Cognitive Impairment Patients," in *International Conference for Innovation in Biomedical Engineering and Life Sciences*, 2016, pp. 82-85.
- [29] Z. German-Sallo and C. Ciufudean, "Waveform-adapted wavelet denoising of ECG signals."
- [30] A. Shoeb and G. Cliord, "Chapter 16 - Wavelets; Multiscale Activity in Physiological Signals," in *Biomedical Signal and Image Processing*, ed, 2005.
- [31] J. Escudero, R. Hornero, D. Abásolo, and A. Fernández, "Blind source separation to enhance spectral and non-linear features of magnetoencephalogram recordings. Application to Alzheimer's disease," *Medical engineering & physics*, vol. 31, pp. 872-879, 2009.
- [32] J. Escudero Rodríguez, "Applications of blind source separation to the magnetoencephalogram background activity in alzheimer's disease," Universidad de Valladolid, 2010.
- [33] R. Hornero, J. Escudero, A. Fernández, J. Poza, and C. Gómez, "Spectral and nonlinear analyses of MEG background activity in patients with Alzheimer's disease," *Biomedical Engineering, IEEE Transactions on*, vol. 55, pp. 1658-1665, 2008.
- [34] J. S. Richman and J. R. Moorman, "Physiological time-series analysis using approximate entropy and sample entropy," *American Journal of Physiology-Heart and Circulatory Physiology*, vol. 278, pp. H2039-H2049, 2000.
- [35] D. E. Lake, J. S. Richman, M. P. Griffin, and J. R. Moorman, "Sample entropy analysis of neonatal heart rate variability," *American Journal of Physiology-Regulatory, Integrative and Comparative Physiology*, vol. 283, pp. R789-R797, 2002.

- [36] H. Azami and J. Escudero, "Improved multiscale permutation entropy for biomedical signal analysis: Interpretation and application to electroencephalogram recordings," *Biomedical Signal Processing and Control*, vol. 23, pp. 28-41, 2016.
- [37] A. Holzinger, M. Hörtenhuber, C. Mayer, M. Bachler, S. Wasserthurer, A. J. Pinho, *et al.*, "On entropy-based data mining," in *Interactive Knowledge Discovery and Data Mining in Biomedical Informatics*, ed: Springer, 2014, pp. 209-226.
- [38] F. C. Morabito, D. Labate, F. La Foresta, A. Bramanti, G. Morabito, and I. Palamara, "Multivariate multi-scale permutation entropy for complexity analysis of Alzheimer's disease EEG," *Entropy*, vol. 14, pp. 1186-1202, 2012.
- [39] E. Ferlazzo, N. Mammone, V. Cianci, S. Gasparini, A. Gambardella, A. Labate, *et al.*, "Permutation entropy of scalp EEG: A tool to investigate epilepsies: Suggestions from absence epilepsies," *Clinical Neurophysiology*, vol. 125, pp. 13-20, 2014.
- [40] C. Bandt and B. Pompe, "Permutation entropy: a natural complexity measure for time series," *Physical review letters*, vol. 88, p. 174102, 2002.
- [41] M. Zanin, L. Zunino, O. A. Rosso, and D. Papo, "Permutation entropy and its main biomedical and econophysics applications: a review," *Entropy*, vol. 14, pp. 1553-1577, 2012.
- [42] N. K. Al-Qazzaz, M. K. Sabir, S. H. B. M. Ali, S. A. Ahmad, and K. Grammer, "Multichannel optimization with hybrid spectral-entropy markers for gender identification enhancement of emotional-based EEGs," *IEEE Access*, vol. 9, pp. 107059-107078, 2021.
- [43] A. Ghaemi, E. Rashedi, A. M. Pourrahimi, M. Kamandar, and F. Rahdari, "Automatic channel selection in EEG signals for classification of left or right hand movement in Brain Computer Interfaces using improved binary gravitation search algorithm," *Biomedical Signal Processing and Control*, vol. 33, pp. 109-118, 2017.
- [44] J. Xiang, X. Han, F. Duan, Y. Qiang, X. Xiong, Y. Lan, *et al.*, "A novel hybrid system for feature selection based on an improved gravitational search algorithm and k-NN method," *Applied Soft Computing*, vol. 31, pp. 293-307, 2015.
- [45] N. V. Chawla, K. W. Bowyer, L. O. Hall, and W. P. Kegelmeyer, "SMOTE: synthetic minority over-sampling technique," *Journal of artificial intelligence research*, pp. 321-357, 2002.
- [46] R. Kohavi, "A study of cross-validation and bootstrap for accuracy estimation and model selection," in *Ijcai*, 1995, pp. 1137-1145.
- [47] Y. Song and J. Zhang, "Discriminating preictal and interictal brain states in intracranial EEG by sample entropy and extreme learning machine," *Journal of neuroscience methods*, vol. 257, pp. 45-54, 2016.
- [48] I. H. Witten and E. Frank, *Data Mining: Practical machine learning tools and techniques*: Morgan Kaufmann, 2005.
- [49] M. Hall, E. Frank, G. Holmes, B. Pfahringer, P. Reutemann, and I. H. Witten, "The WEKA data mining software: an update," *ACM SIGKDD explorations newsletter*, vol. 11, pp. 10-18, 2009.
- [50] L. A. Moctezuma and M. Molinas, "Multi-objective optimization for EEG channel selection and accurate intruder detection in an EEG-based subject identification system," *Scientific Reports*, vol. 10, pp. 1-12, 2020.

## تحسين تصنيف الذاكرة العاملة لنشاط تخطيط الدماغ في الخرف: دراسة مقارنة

نور كمال القزاز \* شوال حميد بن محمد علي\*\*

سي تي أنوم أحمد\*\*\*

\*قسم الهندسة الطبية الحيوية/ كلية الخوارزمي للهندسة/ جامعة بغداد/ بغداد / العراق

\*\*قسم الهندسة الكهربائية والإلكترونية والنظم، كلية الهندسة والبيئة المبنية، جامعة كيبانغسان ماليزيا/ سيلانغور/ ماليزيا

مركز الهندسة الإلكترونية وهندسة الاتصالات المتقدمة/ قسم الهندسة الكهربائية والإلكترونية وهندسة النظم/ جامعة كيبانغسان ماليزيا/ سيلانغور/ ماليزيا

\*\*\*قسم الهندسة الكهربائية والإلكترونية/ كلية الهندسة/ جامعة بوترا ماليزيا/ سيلانغور/ ماليزيا

المعهد الماليزي لبحوث الشيخوخة / جامعة بوترا ماليزيا/ سيردانغ/ سيلانغور/ ماليزيا

\*البريد الإلكتروني: [noorbme@kecbu.uobaghdad.edu.iq](mailto:noorbme@kecbu.uobaghdad.edu.iq)\*\*البريد الإلكتروني: [sawal@ukm.edu.my](mailto:sawal@ukm.edu.my)\*\*\*البريد الإلكتروني: [sanom@upm.edu.my](mailto:sanom@upm.edu.my)

## الخلاصة

لغرض من التحقيق الحالي هو التمييز بين الذاكرة العاملة (WM) في خمسة مرضى يعانون من الخرف الوعائي (VD)، وخمسة عشر مريضاً بعد السكتة الدماغية يعانون من ضعف إدراكي خفيف (MCI)، وخمسة عشر فرداً سليماً للتحكم (HC) بناءً على الخلفية نشاط تخطيط كهربية الدماغ (EEG). تم توضيح التخلص من القطع الأثرية EEG باستخدام التعديل المسبق للموجات (WT) في هذه الدراسة. في الدراسة الحالية، تم استكشاف الإنترنت الطيفية (ApEn)، وإنتروبي التبدل (PerEn)، والإنترنت التقريبية (SpecEn). لتحسين تصنيف WM باستخدام مخطط تصنيف k-أقرب الجيران (kNN)، تم إجراء دراسة مقارنة لاستخدام تحليل الحفاظ على الحي الغامض باستخدام QR-decomposition (FNPAQR) كتقنية لتقليل الأبعاد وتحسين البحث عن الجاذبية الثنائية (IBGSA). تمت زيادة دقة تصنيف kNN من 86.67% إلى 88.09% و 90.52% باستخدام تقنية تقليل الأبعاد FNPAQR وخوارزمية اختيار قنوات IBGSA، على التوالي. وفقاً للنتائج، يعزز IBGSA بشكل موثوق التمييز في WM للمشاركين في HC و MCI و VD. لذلك، توفر WT وميزات الإنترنت و IBGSA ومصنف kNN مؤشراً صحيحاً للخرف للبحث عن نشاط خلفية EEG للمرضى الذين يعانون من VD و MCI.